Recording of the Evoked Potentials During Functional MRI: Applications in Cognitive Neuroscience

F. Kruggel and C.S. Herrmann

Max-Planck-Institute of Cognitive Neuroscience
Stephanstraße 1, D-04103 Leipzig, Germany
email: {kruggel, herrmann}@cns.mpg.de

Abstract

The feasibility of recording event-related potentials (ERP) during functional MRI (fMRI) scanning using higher-level cognitive stimuli was studied. Using responses to illusory figures in a visual oddball task, evoked potentials were obtained with their expected configuration and latencies. A rapid stimulation scheme using randomly varied trial lengths was employed, and class-wise characteristics of the hemodynamic response were obtained by a non-linear analysis of the fMRI time-series. Implications and limitations of conducting combined ERP-fMRI experiments using higher-level cognitive stimuli are discussed.

1 Introduction

Electric potentials and the hemodynamic response of the vascular system are measurable correlates of the brain's neuronal activation. The first effect, measured here by event-related potentials (ERP), is a direct consequence of the electrical activity of neurons, and allows observing the underlying cognitive process on a millisecond timescale. The second effect, measured by here functional magnetic resonance imaging (fMRI) is only indirectly linked to the energy consumption of the neuronal population and takes place on a timescale which is of the order of seconds. However, recent developments in experimental techniques and data analysis have shown that hemodynamic responses are indeed modulated by the experimental stimulation and carry information about the underlying processes at least on a 100 ms timescale [8].

The localization of an activation by ERP source analysis suffers from poor spatial resolution and the theoretical problem of providing only inexact solutions. Here, fMRI is better able to localize brain activations at a high spatial resolution. A combination of both techniques is a very attractive aim in neuroscience, and a number of research groups have taken up the challenge. Most studies so far were performed as separate experiments (i.e. ERP and fMRI recordings at different times), and results were registered and combined by data processing (e.g. [11, 12, 13]). Especially for cognitive stimuli, it is impossible to control whether a subject performs in the same manner in both experiments (e.g., a response may habituate due to stimulus repetition). On the other hand, a combined measurement reveals a number of delicate technical problems: gradients applied during fMRI scanning induce voltages which are much higher than the brain's response and thus interrupt electroencephalogram (EEG) acquisition; the so-called cardio-ballistic effect overlays a pulse-synchronous signal on the EEG, most likely due to pulsation-induced small head and wire movement in the field; electrodes and leads of the EEG setup interact with the fMRI scanning process.

One of the main problems is the low signal-to-noise (SNR) ratio of ERP experiments, which typically require 50-100 repetitions per stimulus class. To obtain a similar ERP quality under the interfering measuring conditions of combined experiments, we estimate that 2-3 times the number of trials must be conducted - even a simple factorial design includes 500-1000 trials. Since the duration of an fMRI experiment (excluding preparatory scans) is typically limited to 45 min, the trial length may not exceed 2.5-5 s, which leads to strongly overlapping hemodynamic responses. Burock *et al.* [3] demonstrated that disentangling responses from rapid presentation rates is possible when using a randomly varied trial length.

The purpose of this study is to demonstrate the feasibility of conducting combined ERP–fMRI experiments under cognitive stimulation. We employ a well-studied cognitive visual oddball task using illusory figures [4, 5]. ERP and fMRI results correspond well with those from previous separate measurements. Benefits and problems of conducting combined experiments are discussed.

2 Experiment and Data Evaluation

Twelve healthy persons took part in this study (5 female, 7 male, mean age 24.8 years, range 22-30 years). Conventional plastic-coated Ag/AgCl electrodes with

iron-free copper leads of 60 cm length were fixed on the subject's scalp by a stretchable plastic cap. Electrodes were mounted at all positions of the international 10/20 system except Pz, where leads left the cap. The reference electrode was placed close to the nasion on the forehead. Cables were twisted pairwise and led through a flexible silicon tube to the EEG amplifier located above the subjects, i.e. head along the body axis in the scanner tunnel. In order to minimize movements, the subject's head was restrained using cushions. Cables and amplifier were fixed to the gantry by tape and weighed down by rice bags.

We used Kanizsa figures and non-Kanizsa figures (see Fig. 1) as stimulus material [4]. Stimuli consisted of either three or four inducer disks which we will consider the shape feature and either constituted an illusory figure (Fig. 1, top) or not (Fig. 1, below). Stimuli were presented for 1000 ms, followed by randomized inter-stimulus-intervals (ISI) of 1000 to 2500 ms. The ISI duration followed an exponential distribution corresponding to $ISI = 1000 - 500 * log(d), d \in [0.04979; 1]$. Figures were displayed in black on a white background with a black fixation cross in the center. Stimuli subtended a visual angle of 4.28 degrees including inducer disks, while the induced illusory figures (Fig. 1, top) subtended 2.86 degrees. Fixation crosses were displayed foveally (0.02 degrees). The ratio of the inducing line ends and the side-length of the illusory figures was 1/4.
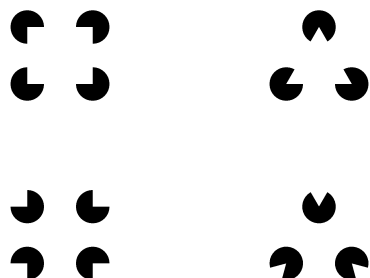

Figure 1: Stimulus material used in the experiment: in the top row, Kanizsa square (KS) and triangle (KT), below: non-Kanizsa square (NS) and triangle (NT).

A block of 20 trials (approx. 50 s) was followed by a 10 s display of the fixation cross alone. Fourty-five blocks were recorded in three experimental runs (a total of 900 trials). Conditions Kanizsa square (KS), Kanizsa triangle (KT), non-Kanizsa square (NS), and non-Kanizsa triangle (NT) were presented equiprobably and randomized across subjects and runs. The Kanizsa square (KS) served as the target condition. Subjects were instructed to press a button with their right middle finger when a target appeared (p = 0.25), and to press another button with the right index finger for all other conditions (p = 0.75).

2.1 EEG Recording and Data Evaluation

A commercially available MR-compatible system (Schwarzer, München, Germany) was used for EEG recording. The battery-powered amplifier located in the scanner tunnel was connected via a 20 m fiber optic link to a standard PC equipped with a digital signal processor (DSP) board in the MR console room. The DSP board received trigger input from the stimulation PC which was recorded with the biosignals. The amplification factor of the system was 10.000 x, with a bandwidth of 0.073-70 Hz. Biosignals were sampled at 500 Hz using an unipolar recording. Collected data were analyzed offline in a series of steps: Slow and high frequency components of the signal were removed using a Hamming-weighted band-pass filter with a pass-band of 0.8-30 Hz. Artifacts from MR gradient pulses were detected in the summed signal. If the slope of this signal exceeded 25 μV/ms, the subsequent interval of 400 ms was marked for exclusion. The cardio-ballistic artifact was corrected by a trial-wise template-based approach described in detail elsewhere [9]. Finally, the corrected EEG was averaged across subjects in a period of -100 to +600 ms relative to stimulation onset, selecting periods with correct responses and specific conditions only.

2.2 fMRI Scanning and Data Evaluation

Functional imaging was performed using a Bruker Medspec 30/100 3.0T MR system. Five slices (TE 30 ms, TR 1500 ms, thickness 6 mm, 2 mm gap, 19.2 cm FOV, 64x64 matrix) were acquired parallel to the AC-PC line in the sagittal plane (approx. at z coordinates -13 mm, -5 mm, +3 mm, +43 mm, +50 mm) by an in-house EPI implementation. The time period during which the images were acquired was 270 ms, leaving a period between 1730 and 3230 ms for EEG acquisition.

Collected fMRI data were analyzed offline in a series of steps: (1) voxelwise correction for the EPI acquisition delay, (2) correction for subject movements in 2D, (3) baseline estimation using a low-pass filter in the temporal domain (cut-off 0.0125 Hz) and subsequent subtraction from the data, (4) detection of functional activation was detected by voxelwise univariate regression analysis. The regression analyses were designed to distinguish (a) task-related activation (KS, KT, NS, NT) from baseline (display of fixation cross alone), (b) target (KS) vs. non-target (KT, NS, NT) related activation, (c) activation related to Kanizsa (KS, KT) vs. non-Kanizsa figures (NS, NT), and (d) activation related to squares (KS, NS) vs. triangles (KT, NT). In all designs, the first two time steps of each stimulus and baseline period were excluded from analysis as transition phases. In addition, the first 5 time steps of each scan were excluded due to their magnetical non-equilibrium. The design matrix was shifted by 5.5 s to match the lag of the hemodynamic response. (5) The F-scores obtained

were corrected for the effective degrees of freedom by analyzing the temporal autocorrelation and converted into z-scores. (6) Z-score maps were registered with a T_1-weighted high resolution MR data set of the same subject and transformed into Talairach space, and averaged within the subject group. (7) The resulting z-score map was thresholded by 4 and activated regions were assessed for their significance on the basis of their spatial extent.

To study parameters of the hemodynamic response quantatively, a non-linear regression model was adapted to the time-series [10]. Each hemodynamic response due to a single stimulus is a modeled by a Gaussian function, assuming that each stimulus of a given class elicits the same response, and that subsequent stimuli add linearly [2]. This defines the model of the time-series $y = \sum_s \sum_{t=0}^{t_{max}} (g_{c(s)} * \exp(-((t - l_{c(s)})/d)^2) + o$, where the parameters of the Gaussian function are called g: gain, l: lag, d: dispersion and o: offset. The inner sum models the hemodynamic response due to a single stimulus in the time interval $t \in [0, t_{max}]$ lasting from stimulation onset for an arbitrary time (here, $t_{max} = 12s$). The outer sum runs over all trials s of the experiment, with $c(s) \in \{KS, KT, NT, NS\}$ referring to the stimulus class. Note that the dispersion and the offset were assumed as class-independent.

First, regions-of-interest (ROIs) were determined by computing a regression analysis in single subjects as described above, measuring the effect of stimulation periods (KS, KT, NS, NT) vs. fixation point display. In the resulting individual $z-$score maps, we defined regions of 6 four-connected, suprathreshold ($z \geq 6$) voxels around local maxima and selected those regions, whose position most closely resembled to regions found in the group analysis (see Tab. 1). The time series for a ROI was obtained by averaging voxel intensities at a given time point. Parameters of the model function were optimized using Powell's algorithm. Ten parameters (gain and lag for each class, class independent dispersion and offset) were determined from a time series of 1800 points. For inter-subject comparisons, relative gain values were computed for each subject and each ROI: $rg_c = g_c / \sum_c g_c$. Lag times were normalized by subtracting the individual lag of a ROI within the area striata (AS). For each subject, ROI and stimulus class, we obtained a relative gain (activation strength) and relative lag (time to response maximum). Resulting values were ordered by time and condition. Orderings were determined by computing Student's t tests (single sided, unequal variance, where > corresponds to $p < 0.05$, $\sim$ to $p \geq 0.05$).

3 Results

Reaction times and responses were recorded along with the stimulation. Reaction times for target conditions were significantly higher for target trials (725.3 $\pm$

68.9 ms) than for non-target trials (668.5 $\pm$ 59.2 ms, p < 1e-8). The grand average event-related potentials for all 4 conditions are compiled in Fig. 2. All stimuli evoked the typical P100 and N170 ERP responses. For statistical analysis, ERP amplitudes were pooled into 6 regions: LA (left anterior: Fp1, F3), LC (left central: C3, T3), LP (left posterior: P3, O1), and their homologues on the right side. ERP components were defined by the time intervals 30-60 ms (N50), 70-110 ms (P100), 130-180 ms (N170), and 300-500 ms (P300). Repeated measures ANOVAs with factors topography (anterior, central, posterior), hemisphere (left, right), form (KS, KT, NS, NT) were conducted to assess the effect of the experimental variables on the measured amplitudes.
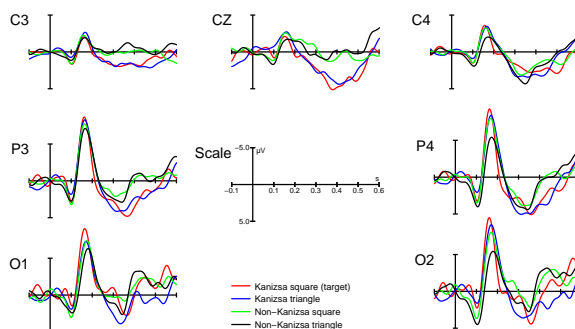

Figure 2: ERPs recorded at six selected positions for the four conditions Kanizsa square (KS, red), Kanizsa triangle (KT, blue), non-Kanizsa square (NS, green), non-Kanizsa triangle (NT, black).

For the N50 component in both posterior regions, square figures elicited a higher amplitude than triangular ones ($F = 50.97, R^2 = 0.168, p < 1e - 12$). No effect was found the the figure factor or the other regions. A similar finding was obtained for the P100 component ($F = 7.8, R^2 = 0.019, p = 0.05$). As might be inferred from Fig. 2, for the N170 component and both posterior regions, a significant ordering of amplitudes by the factor form was found: $KS > KT > NS > NT$ ($F = 31.7, R^2 = 0.182, p < 1e - 12$). Likewise, the same ordering was found for the P300 component ($F = 13.3, R^2 = 0.022, p = 1e - 8$). All results are well in accordance with previous high-resolution ERP [4] and MEG [5] studies.

Selected activation foci of the fMRI group data are compiled in Tab. 1, and shown overlaid onto the group-averaged anatomical data set in Fig. 3.

Results of fMRI data analysis were interpreted as follows:

- During the stimulation (condition KS, KT, NS and NT vs. fixation point) activations are found at expected locations (see Tab. 1 and Fig. 3, top row): the left motor cortex (MCL), the supplementary motor area (SMA), the left and right

Anatomical Location	ROI	Coordinates		
		x	y	z
Motor cortex L	MCL	-38	-19	53
Supplementary motor area	SMA	-5	1	54
Superior parietal lobule L	SPLL	-32	-53	52
Superior parietal lobule R	SPLR	29	-42	44
Middle frontal gyrus L	MFGL	-36	29	32
Middle frontal gyrus R	MFGR	33	45	24
Occ.-mediolateral gyri L	OMGL	-42	-78	11
Occ.-mediolateral gyri R	OMGR	39	-64	6
Precuneus (LR)	PC	5	-33	51
Area striata (LR)	AS	-10	-72	11
Heschl's gyrus L	HGL	-37	-17	- 4
Heschl's gyrus R	HGR	39	-7	- 0

Table 1: Selected activation foci for the all stimuli vs. fixation.

superior parietal lobule (SPLL, SPLR), bilateral occipito-medial (OML, OMR) and occipito-lateral gyri (OLL, OLR). Interestingly, the periphery of the area striata (AS) and Heschl's gyrus is suppressed on both sides. This is interpreted as an attentional focusation on the center of the visual field while suppressing the peripheral visual field and the primary auditory cortex.

- The evaluation of target (KS) vs. non-target (KT, NS, NT) conditions revealed an activation of a bilateral fronto-parietal network (MFGL, SPLL, MFGR, SPLR), and a stronger activation of MCL, SMA and SPL (Fig. 3, second row). The periphery of AS exhibits a relative activation (i.e., a less pronounced suppression).

- Kanizsa figures elicit a stronger activation of MCL and SMA, however less pronounced compared to the target condition. The detection of "meaningful figures" is documented by relatively stronger activations of secondary visual areas (Fig. 3, third row).

- Displaying squares (KS, NS) elicits a stronger activation of MCL, SMA, OMG and OLG than triangles (KT, NT). However, this effect is less pronounced compared to the target effect and the effect elicited by the Kanizsa figures. The periphery of AS is less suppressed, which might be explained by the larger spatial extent of the squares (Fig. 3, bottom).

- In summary, the activation increases in MCL and SMA for squares, Kanizsa figures, and the target condition. OMG and OLG exhibit a stronger activation for squares and Kanizsa figures. SPL appears to be involved in the detection of the target condition. The periphery of AS is suppressed during stimulus display, which is less pronounced for squares and target display.
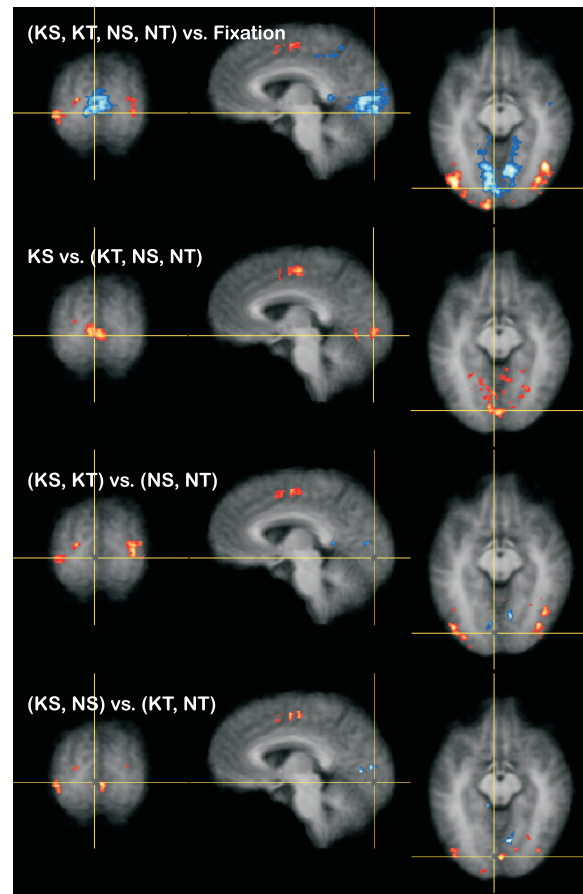

(KS, KT, NS, NT) vs. Fixation

KS vs. (KT, NS, NT)

(KS, KT) vs. (NS, NT)

(KS, NS) vs. (KT, NT)

Figure 3: Color-coded thresholded z-score map ($|z| \in [4; 15]$), overlaid onto the group-averaged anatomical data set which was transformed into Tailarach space. The top row corresponds to the evaluation of all conditions vs. fixation, the second row to the target effect (KS vs. (KT, NS, NT)), the third row to the effect of displaying Kanizsa figures ((KS, KT) vs. (NS, NT)), the bottom row to the effect of displaying squares ((KS, NS) vs. (KT, NT)). Activations are shown in a red-yellow color scale, deactivations in blue-white. Talairach coordinates are compiled in Tab. 1.

- The temporal sequence of activations of ROIs and their mean relative lag was determined as: MCL (-0.019 s) ∼ AS (0.000 s) ∼ OMG (0.034 s) ∼ OLG (0.106 s) < SMA (0.515 s) < SPL (+1.100 s). Three temporal activation groups are discriminated: (AS, OMG, OLG, MCL) appear first, then SMA, then SPL. Activations in ROIs MFGL and MFGR were too low to warrant a proper modelling.

- Lag times for the target condition tended to be greater for the target condition in ROIs SPL ($\Delta t = 0.380$ ms, $p = 0.079$) and SMA ($p = 0.056$), but not in the other ROIs.

- Relative gains vs. experimental conditions were ordered for all ROIs. We obtained for ROI AS: KS ∼ NS ∼ KT ∼ NS, for ROIs OMG, OLG: KS ∼ KT > NT ∼ NS, for ROIs MCL, SMA and SPL: KS > NT ∼ KT ∼ NS. While the activation of central portions of the striate cortex was independent from the stimulus, a stronger activation was found for Kanizsa figures in OMG and OML. A clear selection of the target was found in ROIs MCL, SMA and SPL.

Taken together, ERP responses in the N50 and P100 time window demonstrated a slightly higher activation for squares than for triangles. This result is consistent with a slightly higher activation of the striate cortex found by the regression models. We argue that this due to that fact that four pac-men lead to a greater change in overall brightness and have a greater spatial extent than displaying only three. During the N170 time window, Gestalt-like properties that emerge from binding individual elements seem to become more relevant. The target effect in AS is probably not due to an early selection mechanism since the early ERPs (N50, P100) do not show a target effect. It is more likely that the striate cortex receives feedback from higher visual areas during a later stage of the selection [11]. A fronto-parietal network is responsible for response selection: Both regions are more strongly activated when comparing target vs. non-target conditions in fMRI. The locations of the BOLD effect which resemble this effect (OMG, OLG) are in accordance with previous fMRI localization of the N170 sources. Similar to results from modelling other fMRI experiments [8, 10], ROIs SMA and MCL, which are responsible for response generation, are activated rather early and show a clearly stronger activation during target trials. The auditory cortex and periphery of AS are suppressed during stimulation.

4 Discussion

The feasibility of recording ERPs during fMRI scanning using cognitive stimuli was demonstrated by recording ERPs with the expected configuration while measuring a typical pattern of BOLD responses. While the possibilities of this new methodology are exciting, a few issues should be remembered when planning such experiments, analyzing their data, and interpreting their results:

Problems of a combined measurement: There are mutual influences of the EEG and MRI measuring process. Our clustered EPI protocol allowed recording 5 functional slices in 250 ms, but the EEG amplifier needed approx. 150 ms to recover from saturation. Thus, a window of 400 ms is lost for each block of scans from the EEG time course. For an average trial duration of 2.5 s here, this compiles to an acceptable "duty cycle" of 84 %. However, if the process under study requires scanning of a larger extent of the brain, this might leave EEG windows left which are too short for a meaningful evaluation.

The cardio-ballistic effect may be corrected by using one of the published methods [1, 9]. Due to their comparatively high magnitude on our 3T scanner, remnants of this artifact are still detectable in the corrected output, which corresponds to a lower SNR ratio in the grand averages. We estimate that 2-3 times the trials of a conventional ERP experiments are needed in a combined EEG-fMRI measurement. Using 20 EEG electrodes and cables resulted in a loss of MR signal which was most noticable in the topmost slices. This is best explained by a shielding effect of the cables, and made the shimming process of the MR scanner tedious. Using this conventional EEG setup, this certainly poses an upper limit for the number of electrodes, most likely not much beyond 20.

Problems of exprimental design: As stated above, the rather low SNR of the grand average forces to design experiments with a rather high number of trials per class (say, at least 100). Most detail about the shape properties of the hemodynamic response is obtained when using rather long trial lengths (say, 12 s or more), so that the overlap of sequential BOLD responses is negligible. Obviously, a compromise between the number of stimulus classes in a factorial (or parametric) design, and the trial length must be made. Here, we applied the rapid stimulation protocol using randomly varied trial lengths [3], and class-wise properties of hemodynamic response were obtained by non-linear regression analysis. Obviously, such rapid presentation is better suited to visual than auditory stimulus material.

Problems of analyzing data: We analyzed measured EEG and fMRI data in a conventional fashion, i.e., each measurement separately. When trying to create a synthesis of the results for ERP and fMRI data analysis, the following physiological response properties must be remembered: ERPs measured on the scalp have a rather low spatial resolution, which is partially due to a spatial low-pass filtering effect of the outer hulls of the brain, and thus correspond to an integral activation of a certain brain region at a given time point. Conversely, the BOLD response may be understood as a (fast) neuronal activation convolved by a (slow) hemodynamic response function. This corresponds to a low-pass filtering effect in time, or: an integral activation over a certain time window at a specific brain location. In addition, it is still unclear to which extent lag times are influenced by a delay in neuronal activation *or* in delivery of oxygenated blood to the response area.

Unique models about the underlying processes involved in a cognitive task may be constructed, when assuming that processes are strictly sequential in time and well-separated in space. While this assumption may ap-

proximately hold for early processing stages (i.e., during stimulus perception), it is well known that later processing stages (i.e., decision making, response generation) require a network of temporally strongly overlapping processes, where even re-activations of certain brain regions are under discussion [11]. Modelling such a network will most likely yield non-unique solutions.

Interesting perspectives are open for performing similar experiments using higher-level cognitive tasks. Observing complementary responses from the same stimulation event on a single subject level is very appealing in order to better understand physiological processes underlying brain activation and the functional organization of the brain.

References

[1] Allen P.J., Josephs O., Turner R. (2000) *A method for removing imaging artifact from continuous EEG recorded during functional MRI.* NeuroImage 12, 230-239.

[2] Buckner R.L., Bandettini P.A., O'Craven K.M., Savoy R., Petersen S.E., Raichle M., Rosen B. (1996) *Detection of transient and distributed cortical activation during averaged single trials of a cognitive task using functional magnetic resonance imaging.* Proceedings of the National Academy of Sciences USA 93, 14878-14883.

[3] Burock M.A., Buckner R.L., Woldorff M.G., Rosen B.R., Dale A.M. (1998) *Randomized event-related experimental designs allow for extremly rapid presentation rates using functional MRI.* Neuroreport 9, 3735-3739.

[4] Herrmann C.S., Mecklinger A., Pfeifer E. (1999) *Gamma responses and ERPs in a visual classification task.* Clinical Neurophysiology 110, 636-642.

[5] Herrmann C.S., Mecklinger A., Pfeifer E. (2000) *Magnetoencephalographic responses to illusory figures: Early evoked gamma is affected by processing of stimulus features.* International Journal of Psychophysiology 38, 265-281.

[6] Herrmann C.S., Bosch V. (2001) *Gestalt perception modulates early visual processing.* Neuroreport 12, 901-904.

[7] Huang-Hellinger F., Breiter H.C., McCormack G., Cohen M.S., Kwong K.K., Sutton J.P., Savoy R.L., Weisskopf R.M., Davis T.L., Baker J.R., Belliveau J.W., Rosen B.R. (1995) *Simultaneous functional magnetic resonance imaging and electrophysiological recording.* Human Brain Mapping 3, 13-23.

[8] Kruggel F, von Cramon DY. (1999) *Modeling the hemodynamic response in single-trial functional MRI experiments.* Magnetic Resonance in Medicine 42, 787-797.

[9] Kruggel F., Wiggins C.J., Herrmann C.S., von Cramon D.Y. (2000) *Recording of the event-related potentials during functional MRI at 3.0 Tesla field strength.* Magnetic Resonance in Medicine 44, 277-282.

[10] Kruggel F., Zysset S., von Cramon D.Y. (2000) *Nonlinear regression of functional MRI data: an item recognition task study.* NeuroImage 12, 173-183.

[11] Martinez A., Anllo-Vento L., Sereno M.I., Frank L.R., Buxton R.B., Dubowitz D., Wong E.C., Hinrichs H., Heinze H.J., Hillyard S.A. (1999) *Involvement of striate and visual cortical areas in spatial attention.* Nature Neuroscience 2, 364-369.

[12] Opitz B., Mecklinger A., von Cramon D.Y., Kruggel F. (1999) *Combining electrophysiological and hemodynamic measures of the auditory oddball.* Psychophysiology 36, 142-147.

[13] Woldorff M.G., Tempelmann C., Fell J., Tegeler C., Gaschler-Markefski B., Hermann H., Heinze H.J., Scheich H. (1999) *Lateralized auditory spatial perception and the contralaterality of cortical processing processing as studied with fMRI and MEG.* Human Brain Mapping 7, 49-66.